

## 9. CLIMATE AND CATCH MODELLING

Figure 9.1 shows the results of modelling the detrended global dT and zonal ACI based on a 55-year period of climate oscillations. The figures indicate that a harmonic with this period length is in good agreement with the past oscillations of both dT and ACI, and suggest that similar cyclic changes are likely to continue during the future 30–60 years.

Figure 9.2 shows the temperature dynamics reconstructed from the Greenland ice cores data for the last 400 years combined with the detrended dT dynamics, calculated from the time series of directly measured temperature for the last 150 years (Figure 9.3). It is clear that the dynamics of the measured temperatures for 1861–1975 coincide with the reconstructed Ice Core dT dynamics. With a 55-year period length, the projected model curve is in good agreement with the observed fluctuations of both reconstructed and measured dT.

These data illustrate a good general similarity between the curves of measured and reconstructed temperature time series for the last millennium. There are many reasons to suppose that the climate periodicity, which has lasted over many decades, will remain similar for the next 30 years.

The scheme presented in Figures 9.1–9.3 is applied to forecast commercial catches of two basic groups of fish species: (1) those correlated with the dynamics of the zonal ACI ("zonal-dependent" species) and (2) those correlated with the dynamics of meridional ACI ("meridional-dependent" species) (see Figure 3.6). "Zonal" and "meridional" circulation epochs coincide in phase with the long-term increase and decrease of global temperature, respectively (Lambeck 1980).

Figures 9.4 - 9.14 show the model-generated catches of 12 major commercial species (excluding Peruvian anchovy). The graphs were developed using three basic periods of the climate cycles: 55, 60, and 65 years. In general, all three graphs are in good correspondence with the past catch cycles. The catch trends of Atlantic and Pacific herring, and Atlantic cod fit best to the 55-year periodicity compared to the periods of 60 and 65 years.

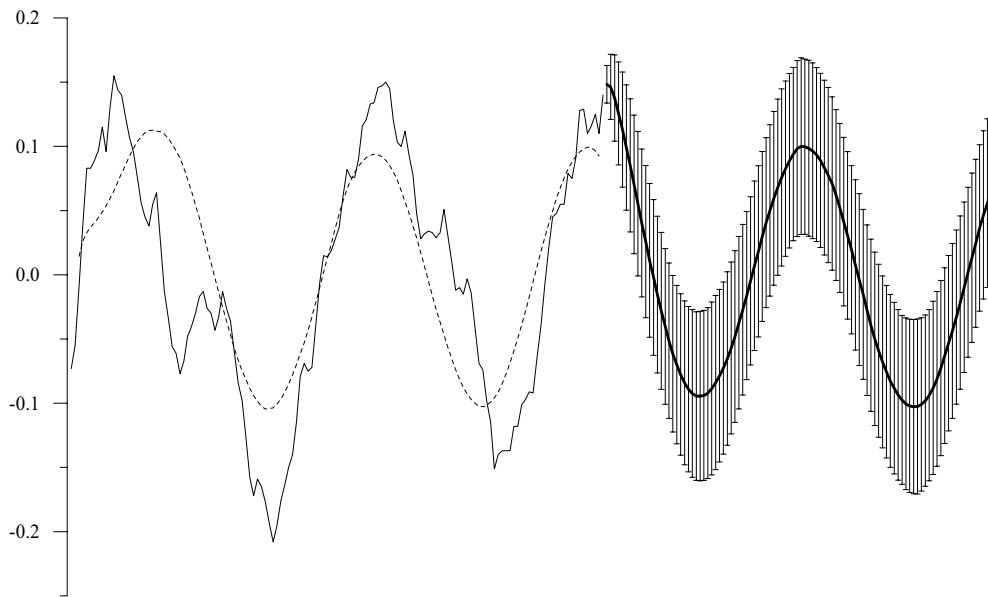
The model-generated forecast of commercial catches (Tables 9.1 and 9.2) is based on the following assumptions:

- 1) Catch dynamics correspond to the smooth "model" curve shown in Figures 9.4 - 9.14.
- 2) Average catch in the maximum of the forecasted cycle corresponds to that in the maximum of the previous cycle. That is, if average catch of Atlantic cod in the mid 1960s was about 3 million tons, then the forecasted catch in the mid-2020s will also be about 3 million tons.

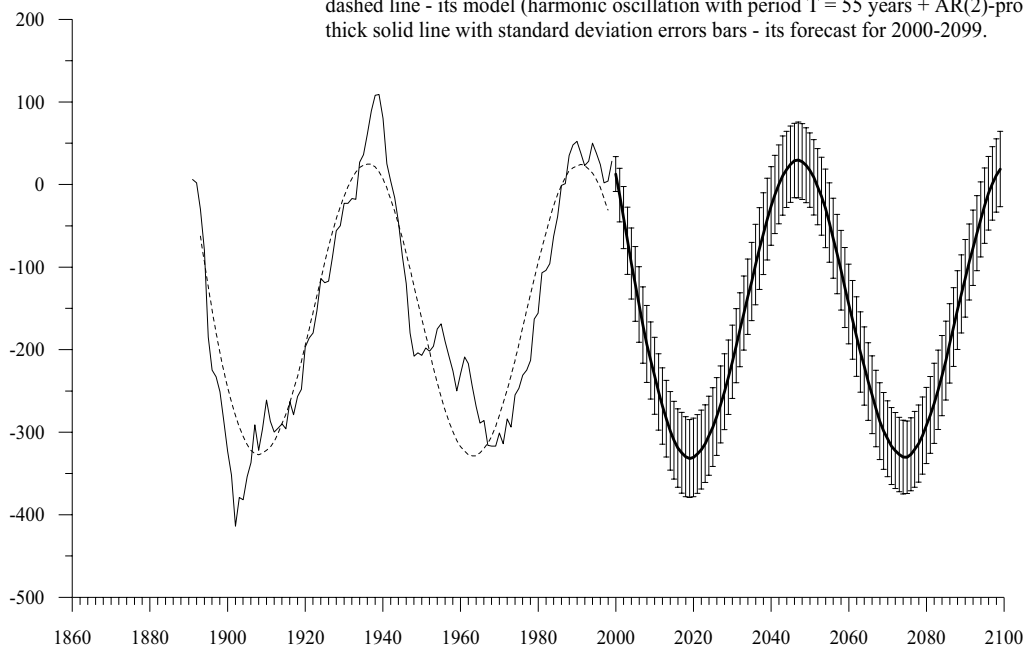
### 9.1 MODELLING OF THE CATCH DYNAMICS OF "MERIDIONAL-DEPENDENT" FISH SPECIES

Figures 9.4 - 9.7 show the model-generated catch dynamics of Atlantic herring and cod, Pacific herring and South African sardine. Excluding stock dynamics of Peruvian anchovy (considered separately in Chapter 10), the catch trends of four "meridional-dependent" species have already passed a depression in the 1980s, and, in line with the climatic trend, both population and catches of these species have been increasing since the mid 1990s. Judging by the past climate cycles, the catch maxima of these species is likely to fall on the middle of the next decade.

Thin solid line -  $\Delta T$  (global temperature anomaly), 1861-1998,  
dashed line - its model (harmonic oscillation with period  $T = 55$  years + AR(2)-process)  
thick solid line with standard deviation errors bars - its forecast for 1999-2099.



Thin solid line - ACI\_WE (atmospheric circulation index (zonal)), 1891-1999,  
dashed line - its model (harmonic oscillation with period  $T = 55$  years + AR(2)-process)  
thick solid line with standard deviation errors bars - its forecast for 2000-2099.



3) 1860 1880 1900 1920 1940 1960 1980 2000 2020 2040 2060 2080 2100

Figure 9.1 The future fluctuations of detrended Global temperature anomaly (top) and “zonal” form of Atmospheric Circulation Index (bottom).

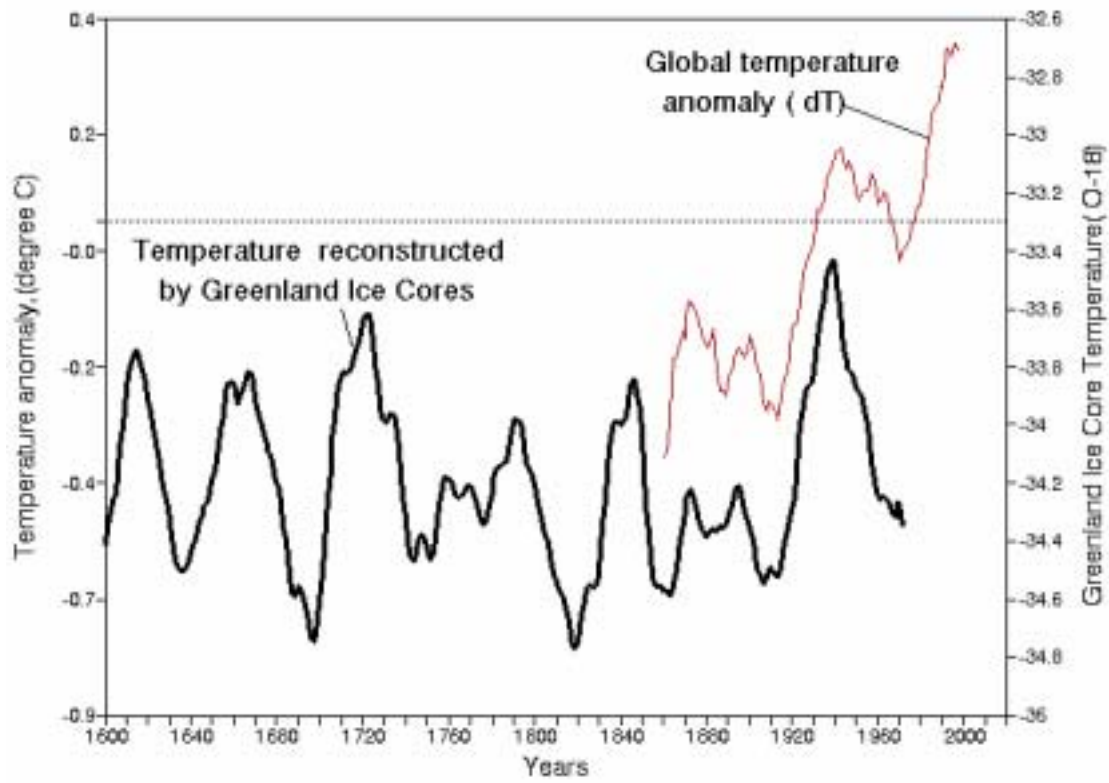


Figure 9.2. A comparison of global temperature anomalies ( $dT$ ) with the temperature dynamics reconstructed from Greenland Ice Cores (Ice Core  $dT$ ).

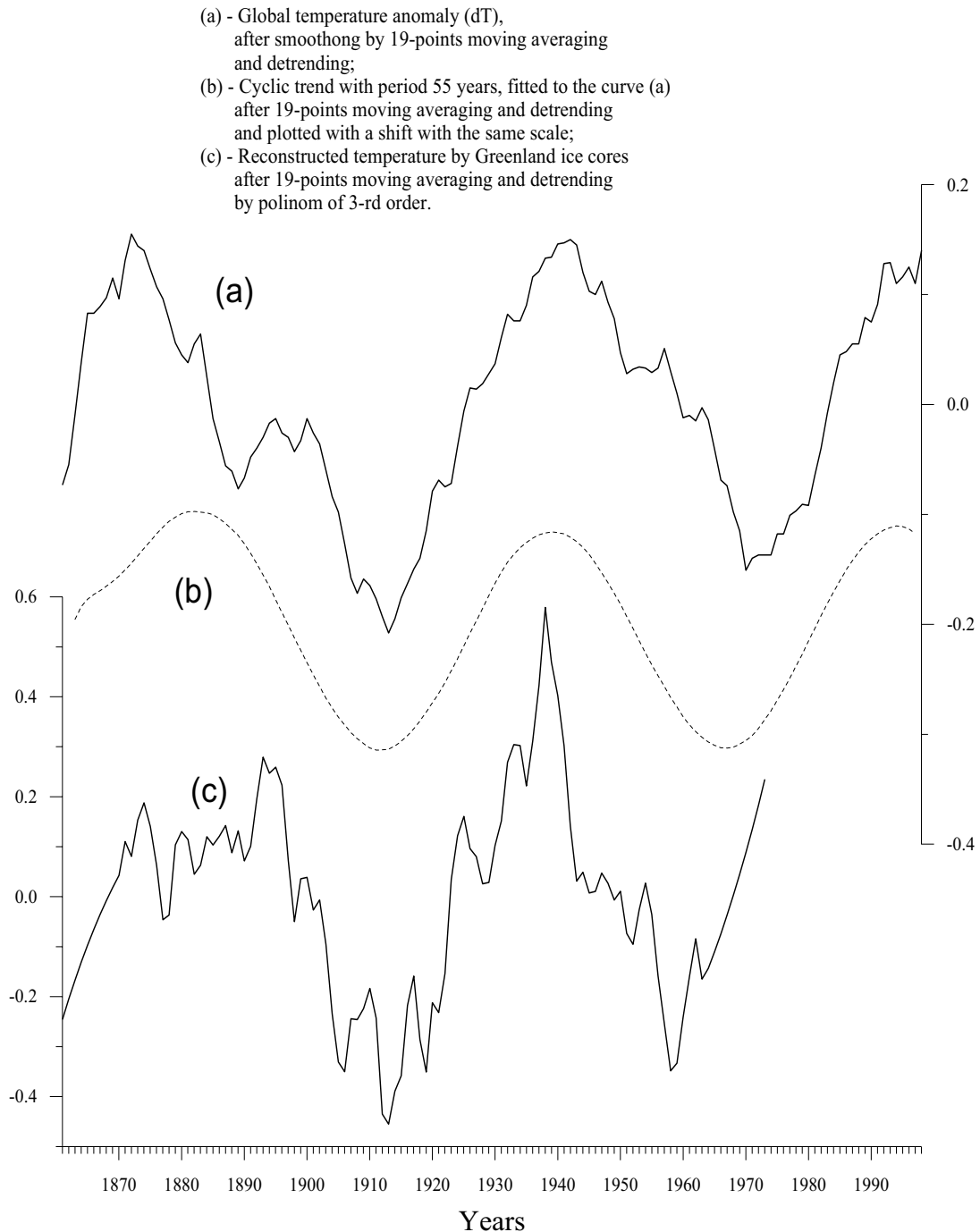


Figure 9.3 A comparison of the detrended global temperature anomaly (dT), the modelled 55-year period climate oscillation curve and the detrended reconstructed ice cores temperature (Ice Cores dT).

The peak of Atlantic cod is shifted by 5 - 7 years to the right (i.e. delayed) from the corresponding peak of Atlantic herring, which is characteristic also for the past dynamics of both species.

Thus, the catch cycles of the four "meridional-dependent" species look as follows: a minimum in the beginning and mid-1980s increasing to the mid-1990s, slowing down in the 2010s to a maximum in 2015–2025, and decreasing from 2025 to a new minimum in the mid-2030s. Catch forecasting for the next 30-years is of the greatest importance for our purposes, although the catch dynamics beyond the 2030s is also of interest (Table 9.1).

**Table 9.1 Model-generated commercial catches (million tons) of meridional-dependent" species in 2005–2040**

Years	Atlantic Herring	Atlantic cod	Pacific herring	South African Sardine
2005	2.2	1.5	0.60	0.30
2010	2.5	2.0	0.65	0.50
2015	3.0	2.5	0.70	0.70
2020	2.5	3.0	0.70	1.00
2025	2.0	3.5	0.75	0.60
2030	1.5	2.8	0.65	0.40
2035	1.2	2.3	0.50	0.35
2040	1.0	1.7	0.35	0.20

## 9.2 MODELLING OF THE CATCH DYNAMICS OF "ZONAL-DEPENDENT" FISH SPECIES

Figures 9.8 - 9.14 show the model-generated dynamics of catch fluctuations for Japanese, Californian, Peruvian, and European sardines, Pacific salmon, Alaska pollock, and Chilean jack mackerel. All seven species are in close correlation with "zonal" ACI, and now exhibit decreases in population and catches, though each are at different stages of the depression. For example, the catch dynamics suggests that Japanese, Peruvian, and European sardine, and Alaska pollock have passed the point of maximum stock and started to decrease in the mid to late 1980s. The catch is forecast to reach its minimum by the mid 2010s, followed by the new increase to a maximum in the early 2040s. As to the other species of this group, the maximum catch of Pacific salmon lags behind the corresponding maximum of Japanese sardine by almost 10 years (in the mid-1990s), followed by gradual decrease (Klyashtorin 1997, 1998). Similar dynamics are characteristic of Californian sardine and Chilean jack mackerel. The model predicts a minimum population of these three species in the 2010s, to be followed by a gradual increase to the maximum in the mid-2040s. The model-generated dynamics of "zonal-dependent" species are presented in Table 9.2.

Thus, cyclic catch fluctuations of "zonal-dependent" species looks as follows: a maximum in the mid-1980s, then a decrease in the early 2000 to a minimum around 2015, followed by a gradual increase in the mid-2020s leading to a new maximum in the 2040s.

**Table 9.2 Model-generated commercial catches (million tons) of "zonal- dependent" species in 2005–2040.**

Years	Japanese sardine	Peruvian Sardine	European sardine	Alaska pollock	Californian sardine	Pacific Salmon	Chilean jack mackerel
2005	0.10	0.25	0.50	2.5	0.25	0.70	2.0
2010	0.05	0.05	0.40	2.0	0.10	0.50	1.5
2015	0.05	0.05	0.30	2.0	0.05	0.35	0.5
2020	0.30	0.10	0.30	2.2	0.02	0.35	0.5
2025	1.00	0.50	0.40	2.5	0.05	0.40	0.7
2030	2.50	1.50	0.80	3.5	0.10	0.50	1.0
2035	3.50	2.50	1.00	4.5	0.25	0.60	1.5
2040	4.50	3.50	1.20	6.0	0.35	0.70	2.5

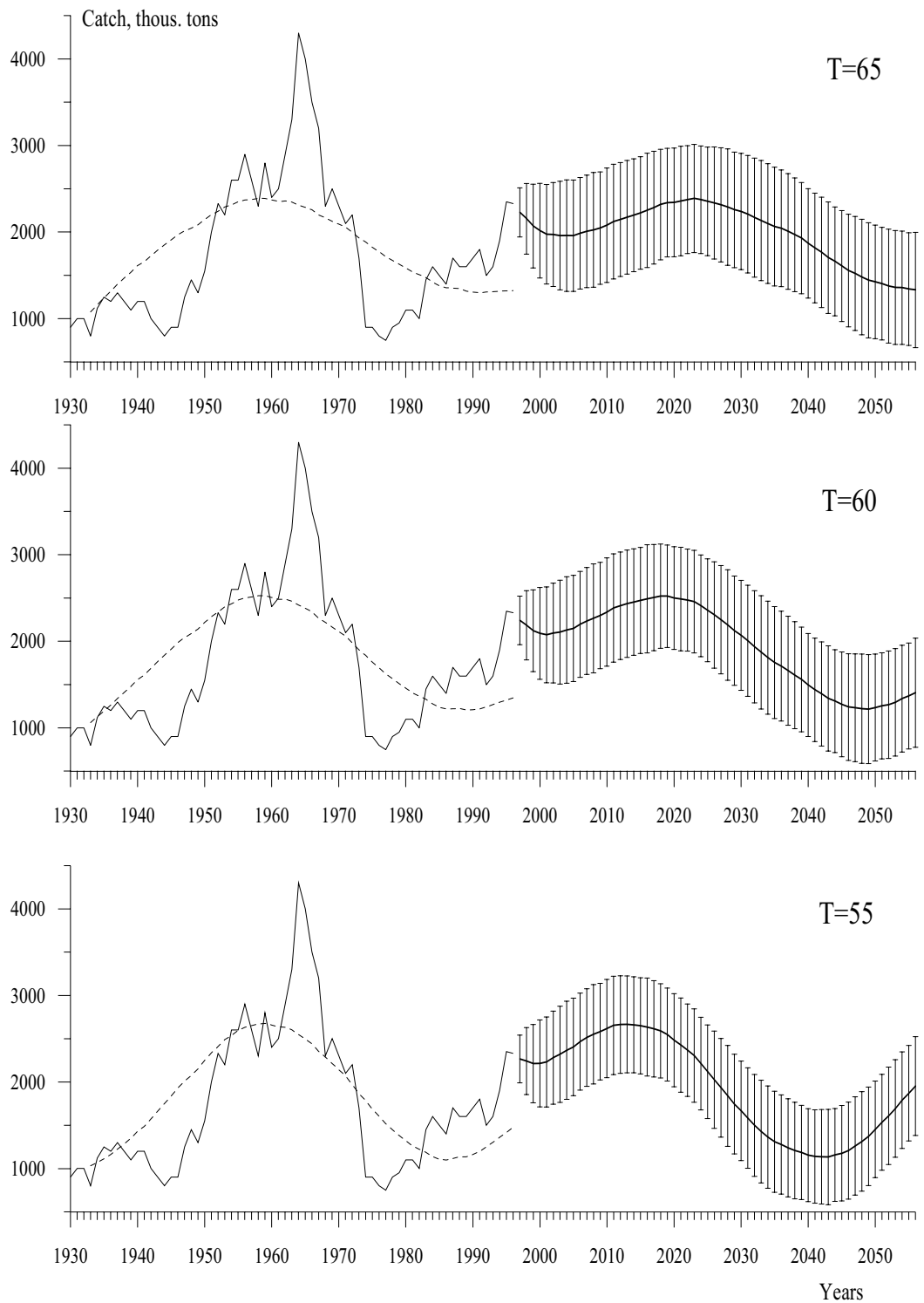


Figure 9.4

Thin solid line - Atlantic herring catch, 1930-1996, thick solid lines with standard deviations error bars - mean value for 1000 bootstrap realizations for 1997-2056 for different periods  $T$  (years) of cyclic trend, dashed line - mean value for 1000 bootstrap realizations for 1933-1996.

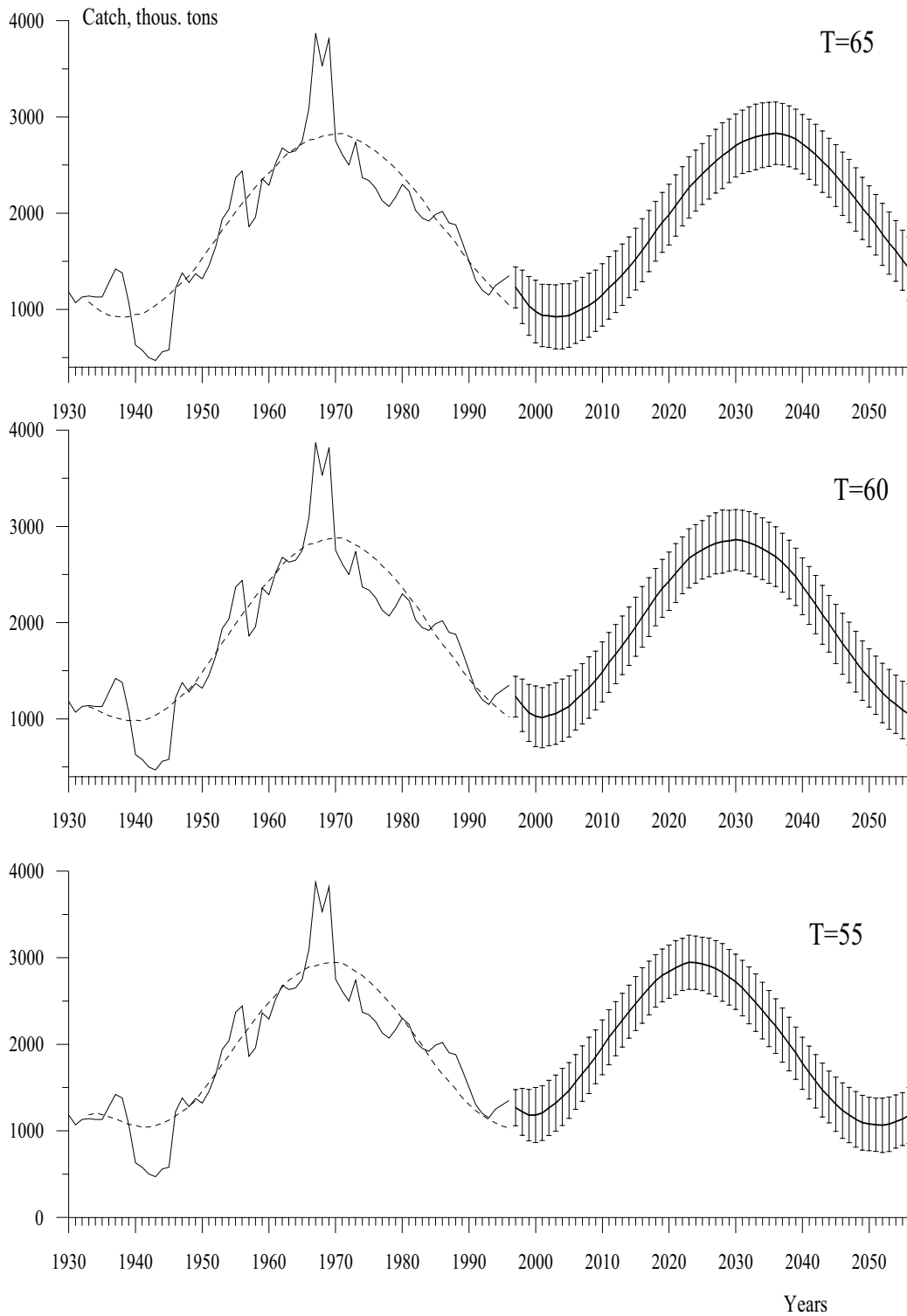


Figure 9.5 Thin solid line - Atlantic cod catch, 1930-1996, thick solid lines with standard deviations error bars - mean value for 1000 bootstrap realizations for 1997-2056 for different periods  $T$  (years) of cyclic trend, dashed line - mean value for 1000 bootstrap realizations for 1933-1996.

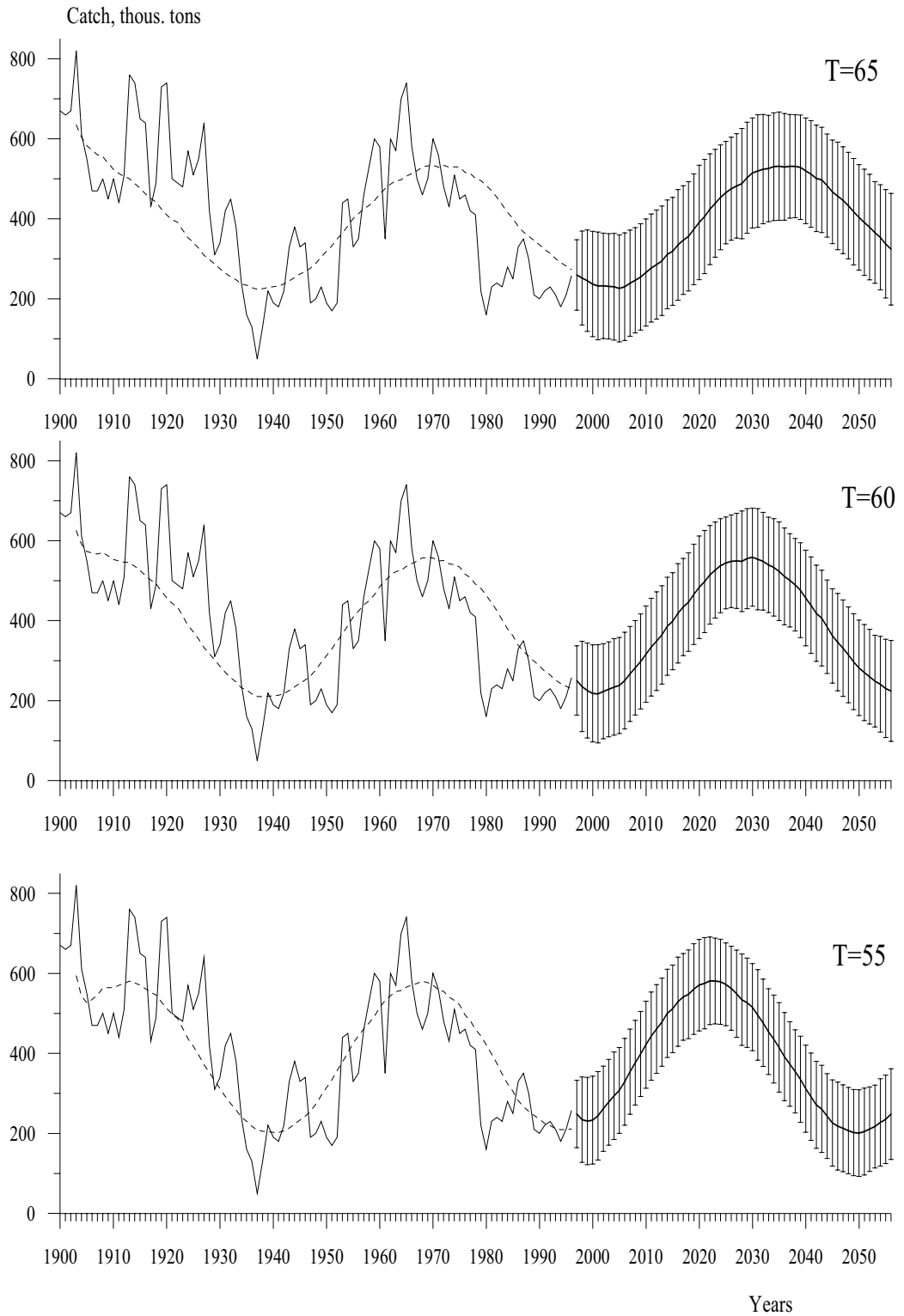


Figure 9.6 Thin solid line - Pacific herring catch, 1900-1996, thick solid lines with standard deviations error bars - mean value for 1000 bootstrap realizations for 1997-2056 for different periods  $T$  (years) of cyclic trend, dashed line - mean value for 1000 bootstrap realizations for 1903-1996.



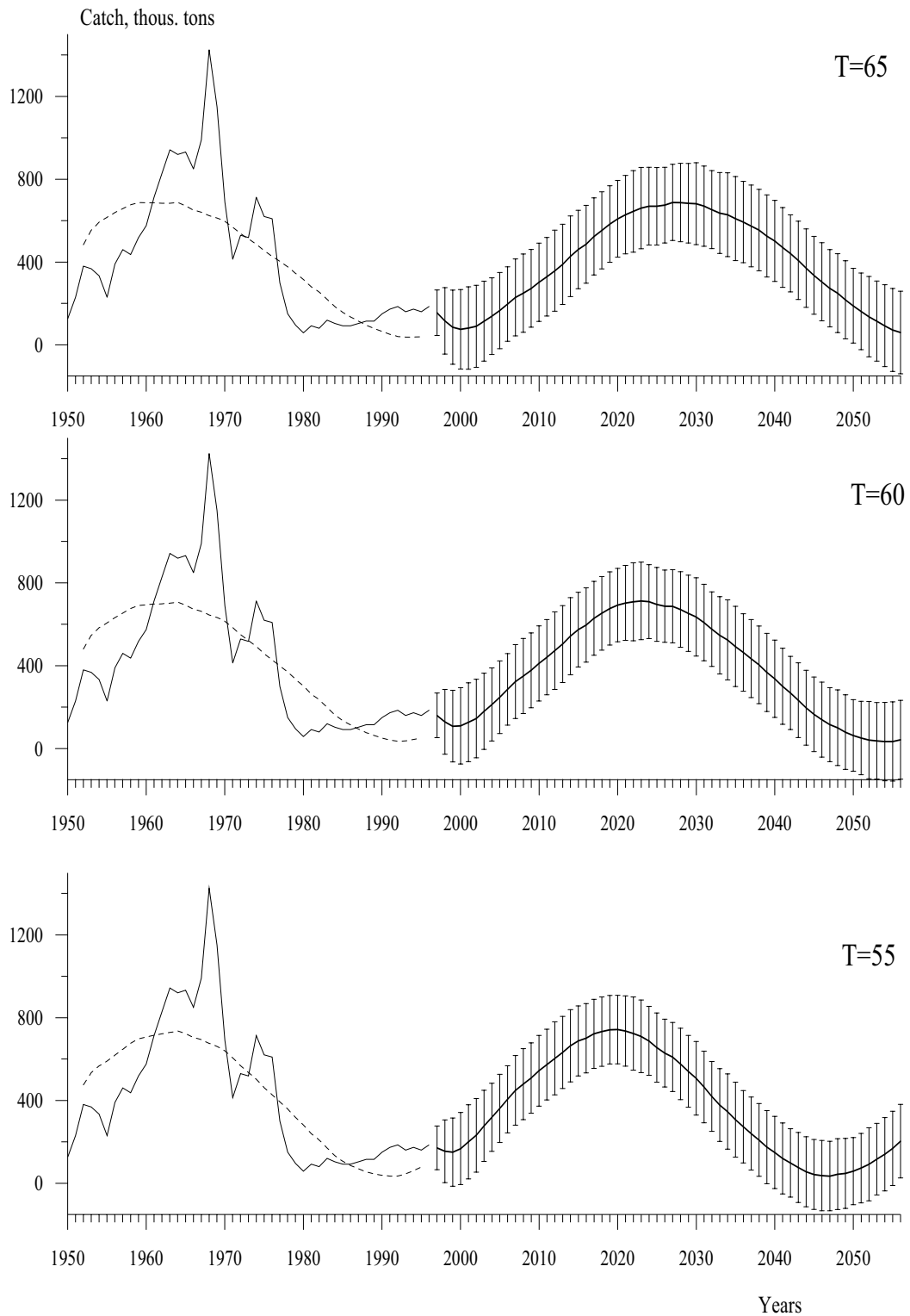


Figure 9.7 Thin solid line - South African sardine catch, 1950-1996, thick solid lines with standard deviations error bars - mean value for 1000 bootstrap realizations for 1997-2056 for different periods  $T$  (years) of cyclic trend, dashed line - mean value for 1000 bootstrap realizations for 1953-1996.

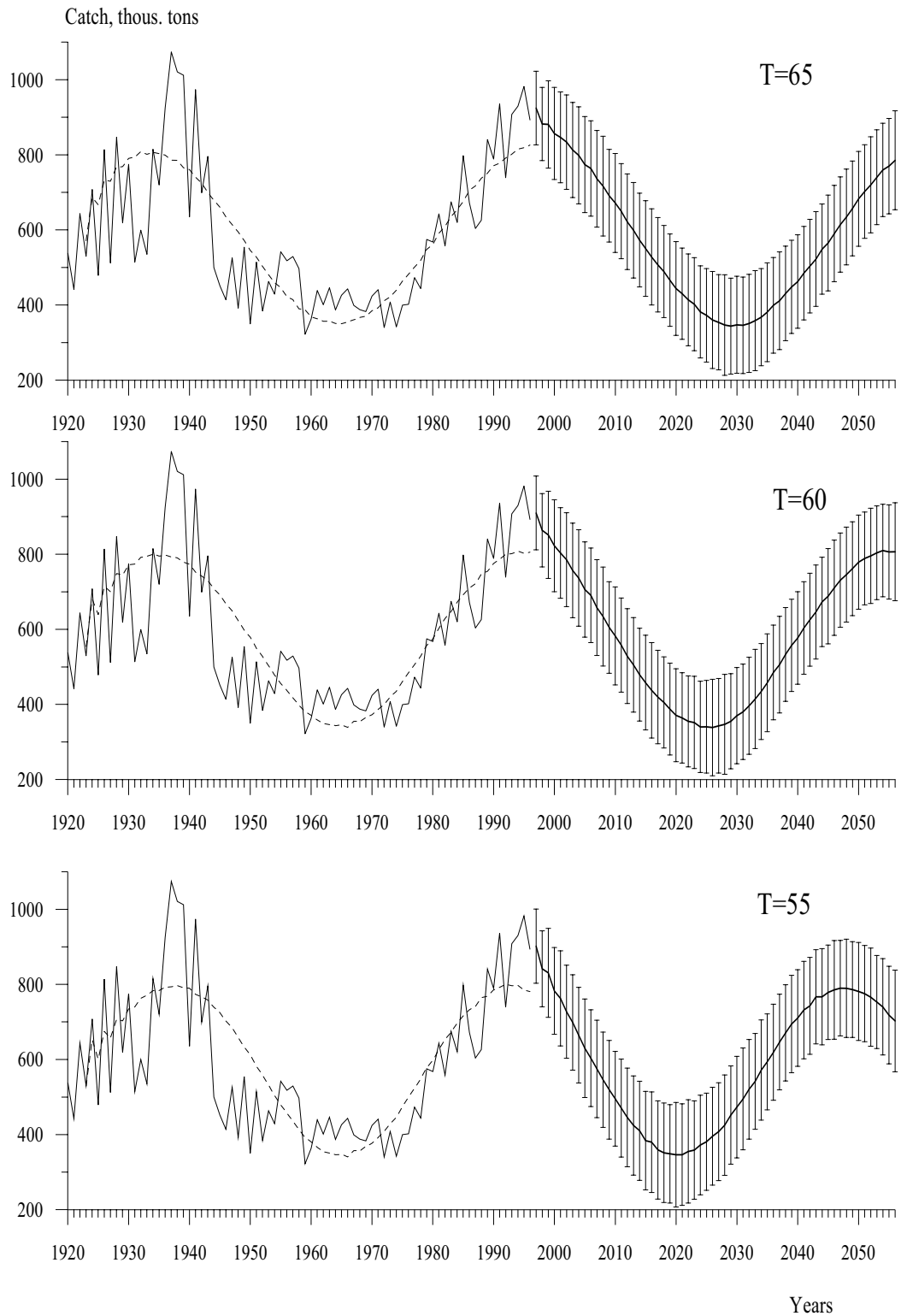


Figure 9.8 Thin solid line - Pacific salmon catch, 1920-1996, thick solid lines with standard deviations error bars - mean value for 1000 bootstrap realizations for 1997-2056 for different periods  $T$  (years) of cyclic trend, dashed line - mean value for 1000 bootstrap realizations for 1923-1996.

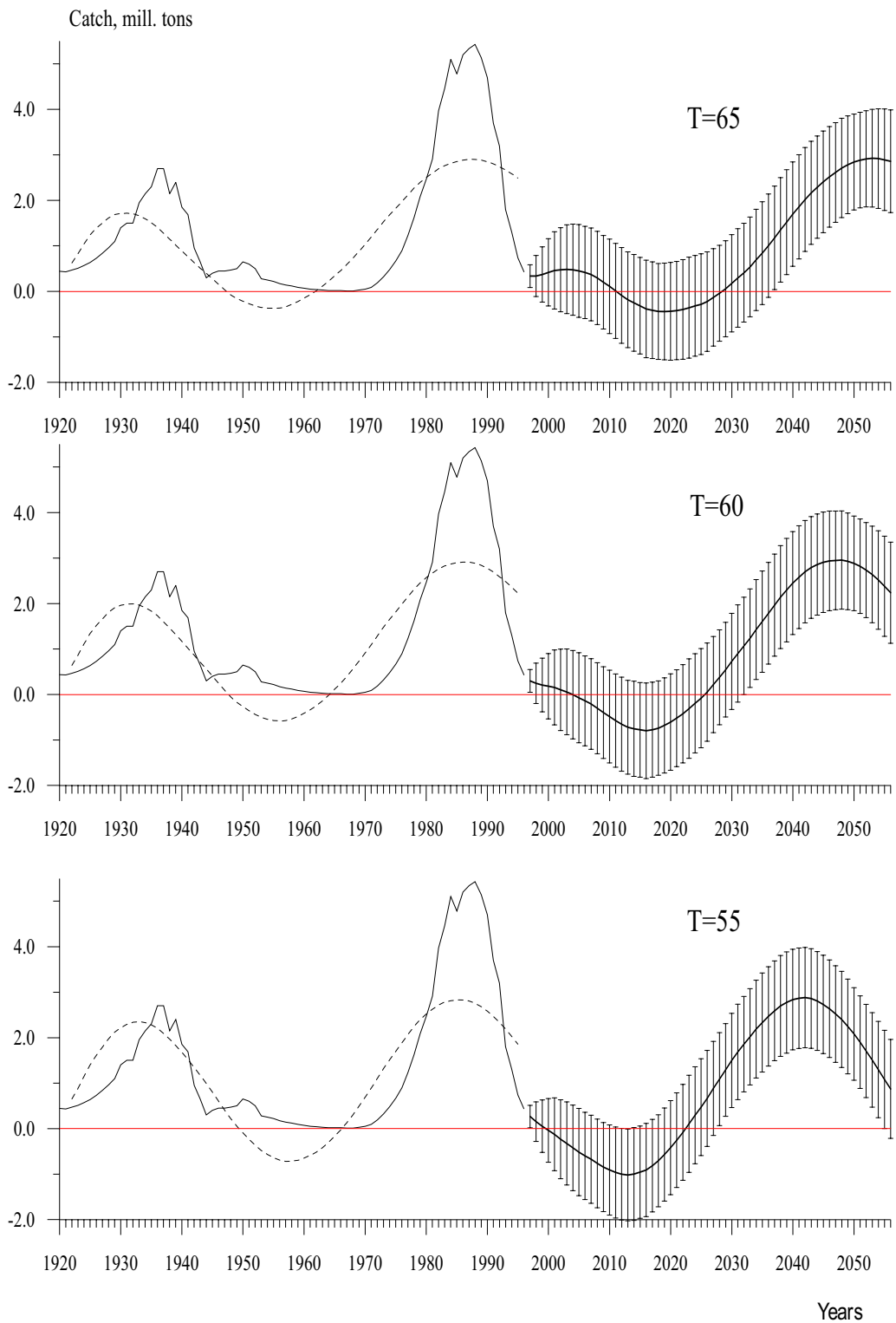


Figure 9.9 Thin solid line - Japanese sardine catch, 1920-1996, thick solid lines with standard deviations error bars - mean value for 1000 bootstrap realizations for 1997-2056 for different periods  $T$  (years) of cyclic trend, dashed line - mean value for 1000 bootstrap realizations for 1923-1996.

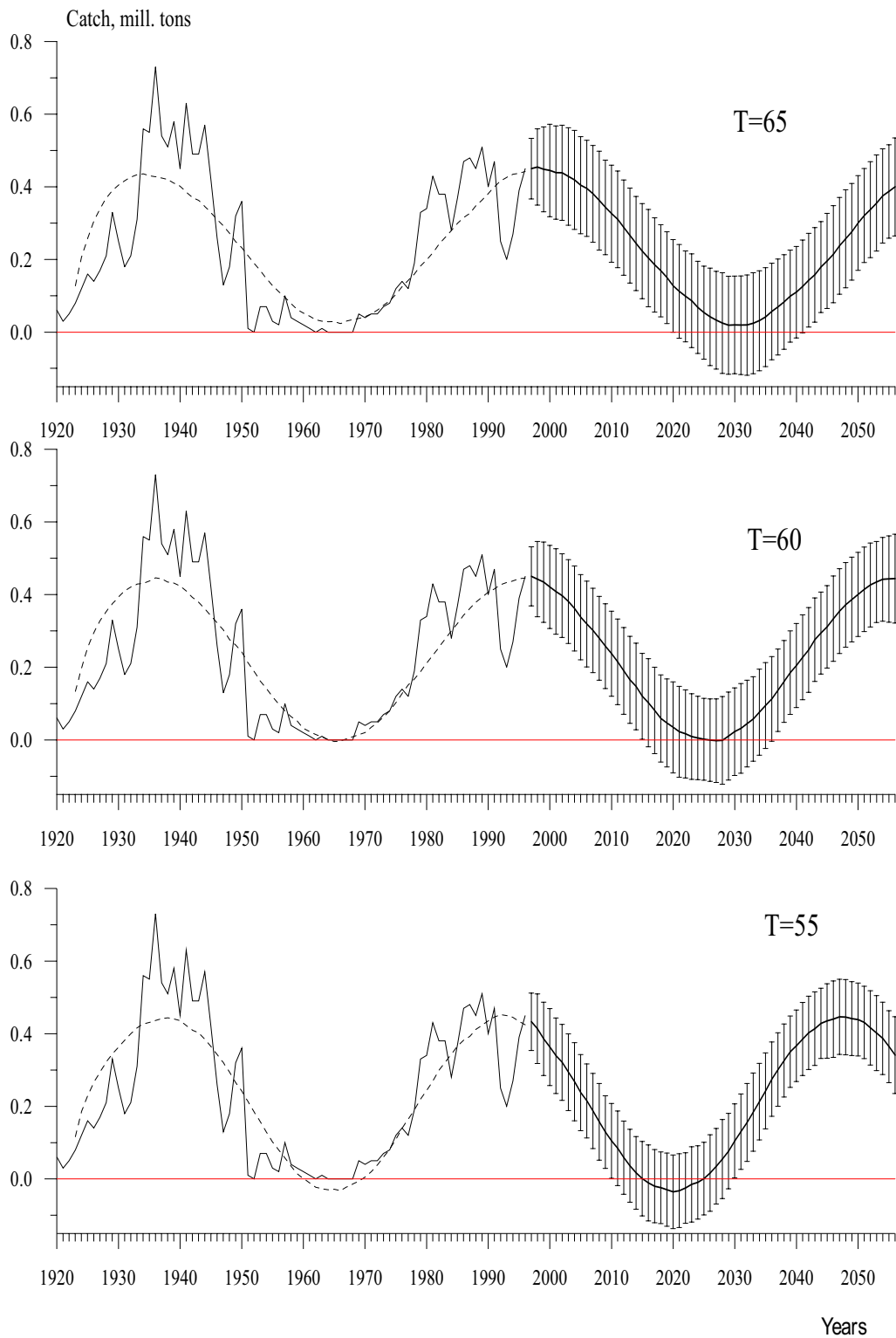


Figure 9.10 Thin solid line - Californian sardine catch, 1920-1996, thick solid lines with standard deviations error bars - mean value for 1000 bootstrap realizations for 1997-2056 for different periods  $T$  (years) of cyclic trend, dashed line - mean value for 1000 bootstrap realizations for 1923-1996.

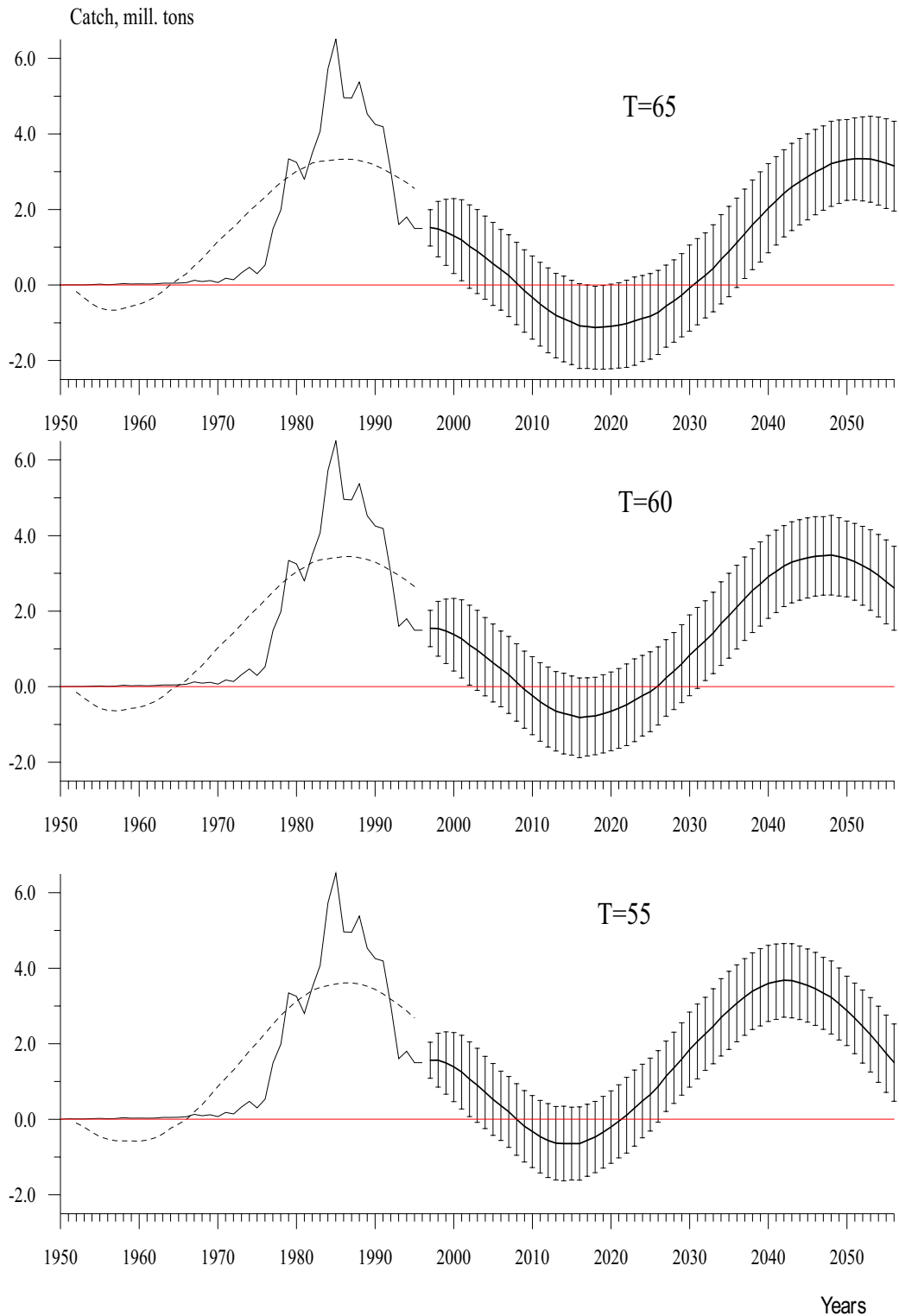


Figure 9.11 Thin solid line - Peruvian sardine catch, 1950-1996, thick solid lines with standard deviations error bars - mean value for 1000 bootstrap realizations for 1997-2056 for different periods  $T$  (years) of cyclic trend, dashed line - mean value for 1000 bootstrap realizations for 1953-1996.

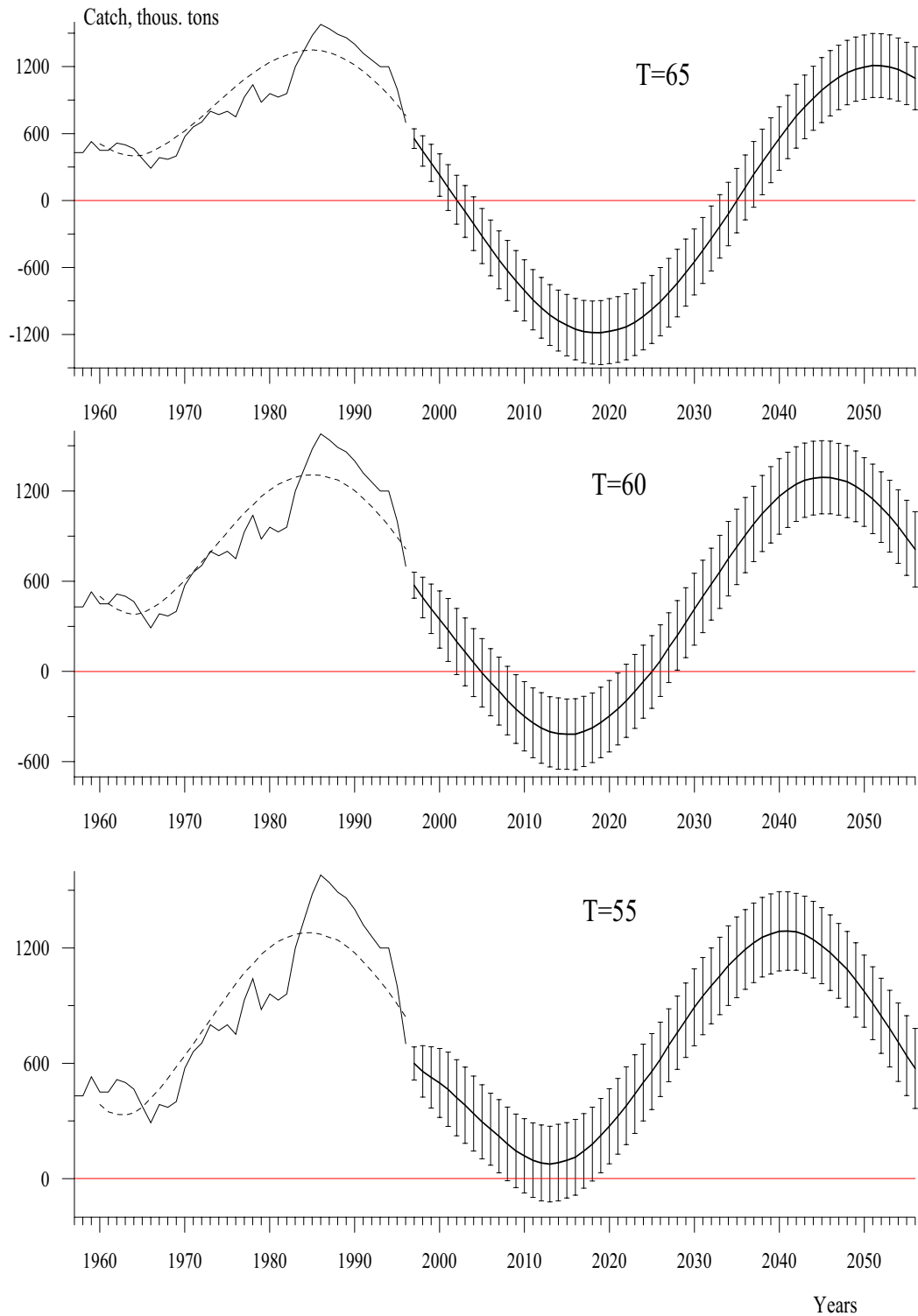


Figure 9.12 Thin solid line - European sardine catch, 1957-1996, thick solid lines with standard deviations error bars - mean value for 1000 bootstrap realizations for 1997-2056 for different periods  $T$  (years) of cyclic trend, dashed line - mean value for 1000 bootstrap realizations for 1960-1996.

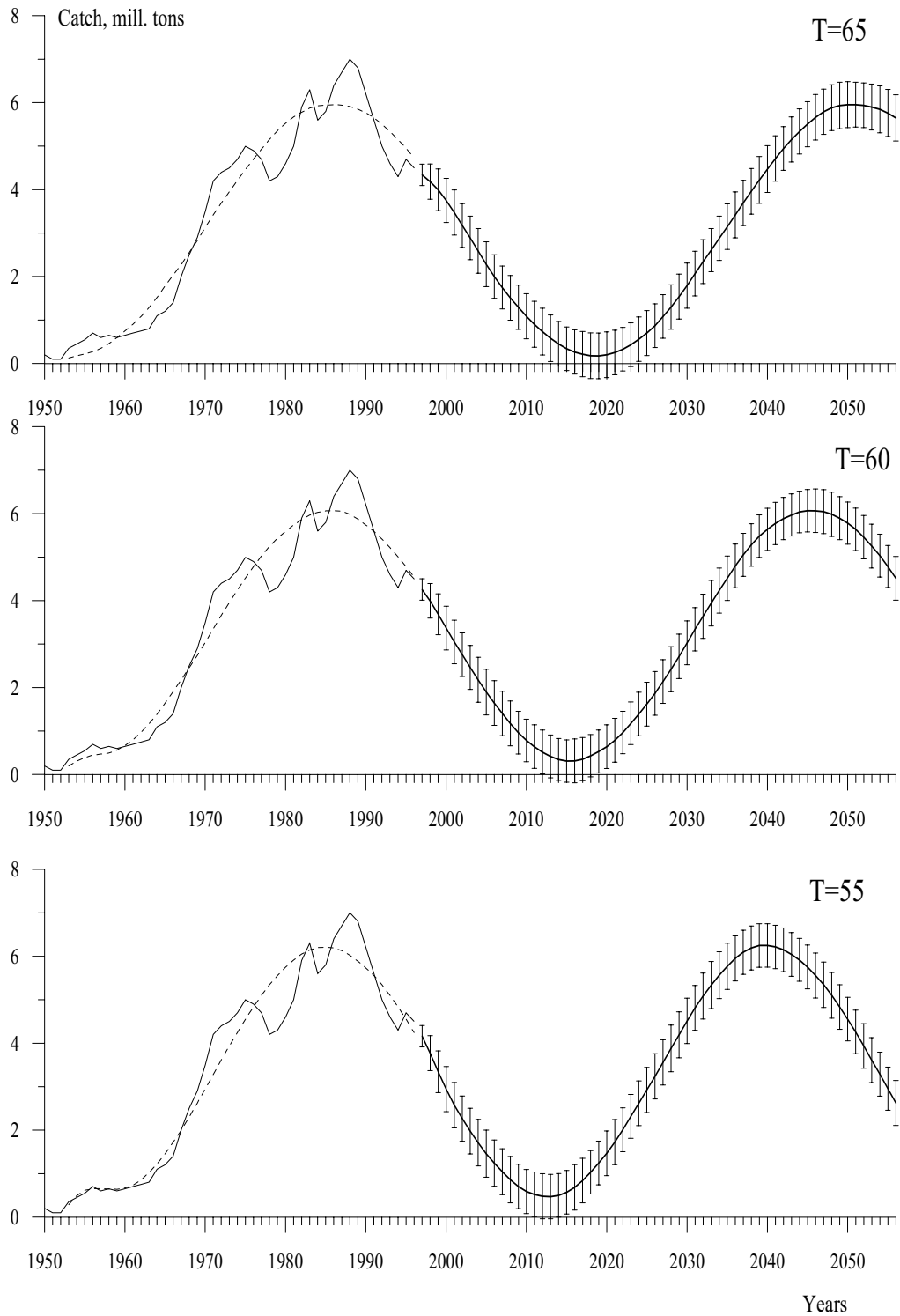


Figure 9.13 Thin solid line - Alaska pollock catch, 1950-1996, thick solid lines with standard deviations error bars - mean value for 1000 bootstrap realizations for 1997-2056 for different periods  $T$  (years) of cyclic trend, dashed line - mean value for 1000 bootstrap realizations for 1953-1996.

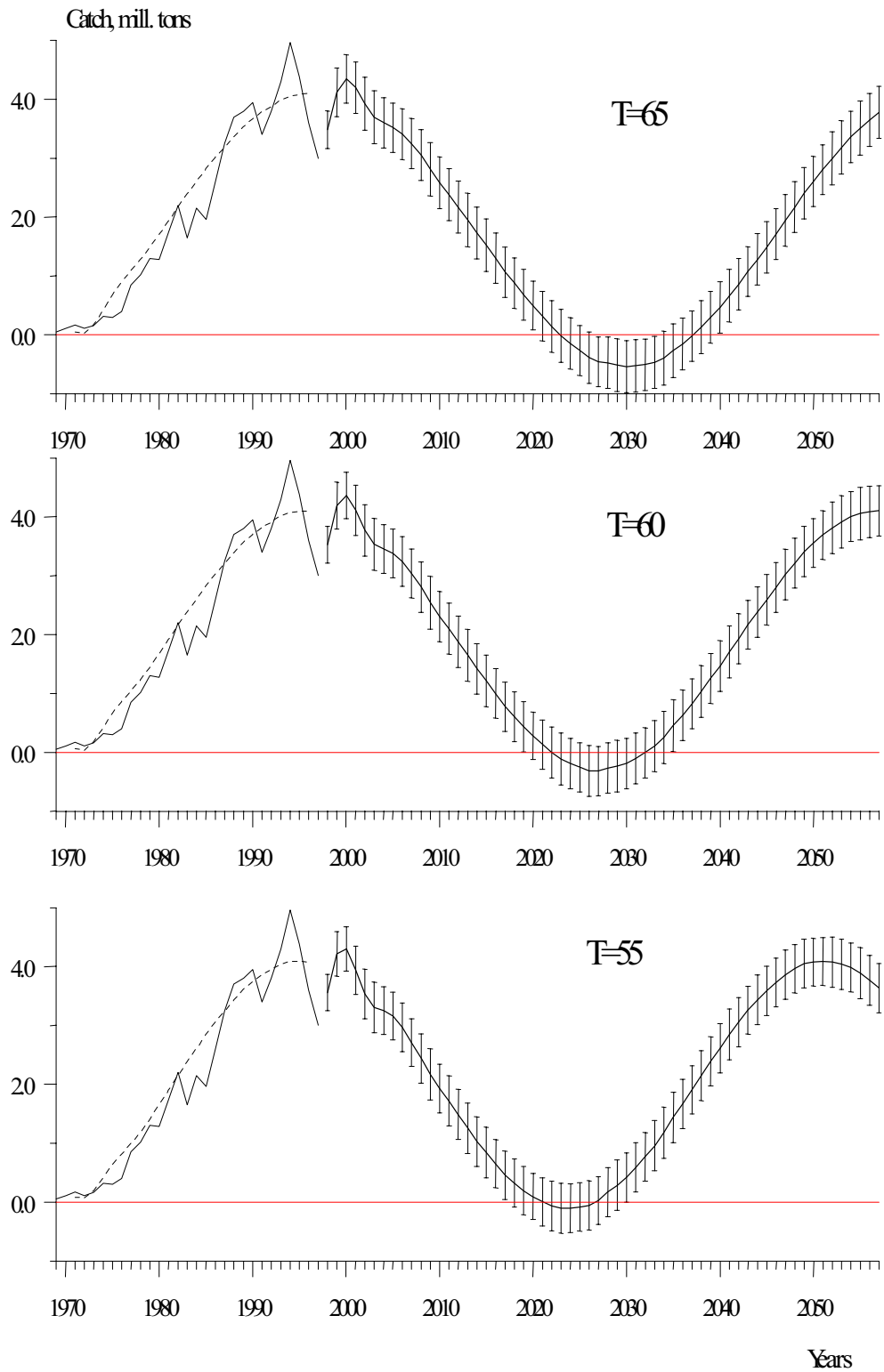


Figure 9.14

Thin solid line - Chilean jack mackerel catch, 1969-1997, thick solid lines with standard deviations error bars - mean value for 1000 bootstrap realizations for 1998-2057 for different periods  $T$  (years) of cyclic trend, dashed line - mean value for 1000 bootstrap realizations for 1971-1997.